



Identification of a non-phosphorylated, cell permeable, small molecule ligand for the Stat3 SH2 domain

Brent D. G. Page^a, Steven Fletcher^a, Peibin Yue^b, Zhihua Li^c, Xiaolei Zhang^b, Sumaiya Sharmeen^d, Alessandro Datti^e, Jeffrey L. Wrana^{e,f}, Suzanne Trudel^c, Aaron D. Schimmer^d, James Turkson^b, Patrick T. Gunning^{a,*}

^a Department of Chemistry, University of Toronto Mississauga, 3359 Mississauga Road, Mississauga, ON, Canada L5L 1C6

^b Department of Molecular Biology and Microbiology, Burnett College of Biomedical Sciences, University of Central Florida, Orlando, FL 32826, USA

^c Princess Margaret Hospital, McLaughlin Centre for Molecular Medicine, 620 University Avenue, Toronto, ON, Canada M5G 2C1

^d Ontario Cancer Institute/Princess Margaret Hospital, 610 University Avenue, Toronto, ON, Canada M5G 2M9

^e Center for Systems Biology, Samuel Lunenfeld Research Institute, Mount Sinai Hospital, Toronto, ON, Canada M5G 1X5

^f Department of Molecular Genetics, University of Toronto, ON, Canada M5S 1A8

ARTICLE INFO

Article history:

Available online 30 June 2011

Keywords:

Stat3
Cancer therapeutics
Jak/Stat pathway
Protein–protein interaction
Inhibitors of apoptosis

ABSTRACT

Signal transducer and activator of transcription 3 (Stat3) protein is a cytosolic transcription factor that is aberrantly activated in numerous human cancers. Inhibitors of activated Stat3–Stat3 protein complexes have been shown to hold therapeutic promise for the treatment of human cancers harboring activated Stat3. Herein, we report the design and synthesis of a focused library of salicylic acid containing Stat3 SH2 domain binders. The most potent inhibitor, **17o**, effectively disrupted Stat3–phosphopeptide complexes ($K_i = 13 \mu\text{M}$), inhibited Stat3–Stat3 protein interactions ($\text{IC}_{50} = 19 \mu\text{M}$) and silenced intracellular Stat3 phosphorylation and Stat3–target gene expression profiles. Inhibition of Stat3 function in both breast and multiple myeloma (MM) tumor cells correlated with induced cell death ($\text{EC}_{50} = 10$ and $16 \mu\text{M}$, respectively).

© 2011 Elsevier Ltd. All rights reserved.

Introduction: As a master regulator of oncogenic cellular processes, signal transducer and activator of transcription (Stat) 3 protein has become the focus of molecularly targeted anti-cancer therapeutic development. Stat3 protein is a cytosolic transcription factor that plays a key role in mediating cell division and apoptosis.^{1,2} Stat3 signaling is initiated by extracellular cytokine³ or growth factor⁴ receptor stimulation and results in the expression of anti-apoptotic proteins that control cell growth and survival.^{2,5} As part of the signaling cascade, Stat3 is recruited to the intracellular domain of the target receptor, where it is phosphorylated on Tyr705.^{6–8} Once phosphorylated, Stat3 dissociates, binds another activated Stat3 monomer through reciprocal Src Homology 2 (SH2) domain–phosphotyrosine interactions and translocates to the nucleus. Once in the nucleus, dimeric Stat3 binds to DNA and promotes the transcription of proteins that govern cell cycling and prevent apoptosis.^{5–8} In healthy cells, Stat3 activity is transient and tightly controlled by suppressors of cytokine signaling, phosphatases and proteasomal degradation.⁹ In many human cancers, however, Stat3 activity is hyperactivated leading to overexpression and accumulation of anti-apoptotic proteins within the cell. Elevated levels of Stat3 activation confer resistance to natural apopto-

tic cues and allows for rapid proliferation and de novo tumorigenesis. Aberrantly activated Stat3 is found in numerous human cancers including leukemia and lymphoma, as well as cancers of the breast, prostate, lung, head, neck, and ovaries.^{2,9–11}

Numerous studies have demonstrated that inhibition of Stat3 activation leads to reduced levels of Stat3–target gene expression profiles and correlates with programmed cell death.^{12–14} To date, effective disruption of Stat3 function has been achieved primarily through inhibition of transcriptionally active Stat3–Stat3 dimers. The Stat3–Stat3 binding complex is characterized by large, non-contiguous intrafacial surface areas possessing few targetable binding sites.¹² As a result, the development of potent small-molecule Stat3 inhibitors remains a challenging task. The majority of published Stat3 inhibitors bind Stat3's phosphopeptide binding SH2 domain (Fig. 1).^{11–13,15–17}

We have recently identified a potent salicylic acid-based Stat3 inhibitor, **7** (SF-1-066⁶ (or 27 h)¹⁸) after a structure–activity relationship (SAR) study of compound **1** (S31-201, Fig. 1). Inhibitor **7** showed promising anti-Stat3 activity both in vitro, disrupting Stat3 protein–phosphopeptide and Stat3–Stat3 protein–protein interactions and elicited in vivo suppression of breast tumor xenografts.¹⁹ Moreover, fluorescence polarization binding experiments showed that **7** is selective for Stat3's SH2 domain *cf.* Stat5 and Stat1 isoforms (Stat3 $K_i = 15 \mu\text{M}$; Stat5, $K_i > 25 \mu\text{M}$; Stat1, $K_i > 25 \mu\text{M}$).

* Corresponding author.

E-mail address: patrick.gunning@utoronto.ca (P.T. Gunning).

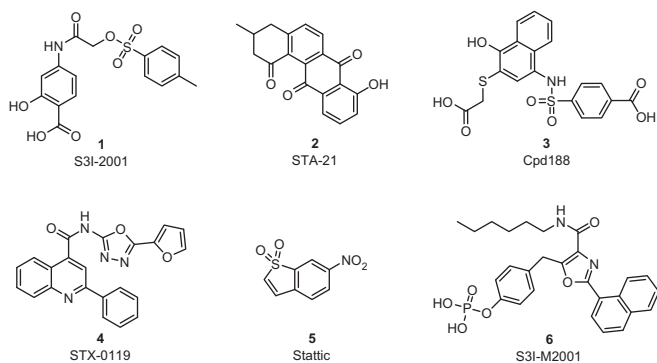


Figure 1. Small molecule Stat3 SH2 domain binders.

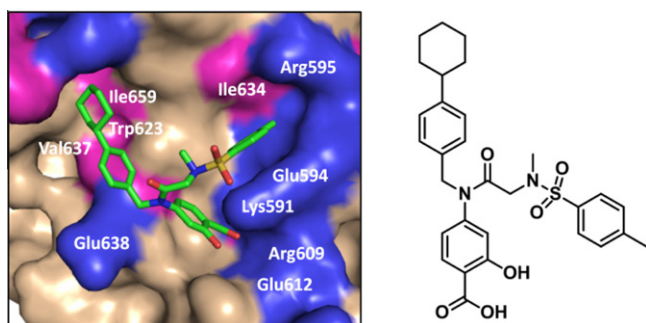


Figure 2. GOLD docking studies of **7** bound to Stat3's SH2 domain.⁶

Encouragingly, **7** showed negligible effects against 'healthy' cells lacking activated Stat3 (NIH3T3, TE-71, and HPDEC) and selectively killed cancer cells harboring aberrant Stat3 activity.¹⁹ GOLD²⁰ docking studies revealed that compound **7** binds to the pTyr-binding portion of the SH2 domain, with the salicylic acid making interactions with Lys591, Glu594 and Arg609.^{6,19} In addition, the hydrophobic cyclohexyl-benzyl appendage forms van der Waal's interactions with a series of predominantly hydrophobic residues (Fig. 2).

In this study we investigated the binding significance of the toluene-sulfonamide substituent to Stat3-SH2 domain recognition. We herein report an SAR of the sulfonamide portion of compound **7**, and present novel analogs, including **17o**, which exhibited improved inhibition of Stat3 function both in vitro and in whole cell tumor models of breast and multiple myeloma cancers.

Materials and methods. *Electrophoretic Mobility Shift Assay:* EMSA analysis was performed as previously reported.^{6,19} Nuclear extracts of NIH3T3/vSrc cells were pre-incubated with varying concentrations of compounds for 30 min at room temperature prior to incubation with ³²P-labeled oligonucleotide probe, hSIE (high affinity sis-inducible element from the c-fos gene, m67 variant, 5'-AGCTTCATTCCCGTAAATCCCTA) for 30 min at 30 °C before subjecting to EMSA analysis. DNA-binding activities were measured for each band at each concentration of inhibitor and quantified using ImageQuant. Results were plotted as percent of control from which an IC₅₀ value could be derived.

Fluorescence polarization assay: As previously reported,^{6,21} fluorescence polarization experiments were performed on an Infinite M1000 (Tecan, Crailsheim, Germany) using black 384-round bottom well plates (Corning), and buffer containing 50 mM NaCl, 10 mM Hepes, pH 7.5, 1 mM EDTA, and 2 mM dithiothreitol and a final concentration of 5% DMSO. Stat3 protein (150 nM) was treated with varying concentrations of inhibitor compounds

(100–0.19 μM final concentrations). The fluorescent probe was added at a final concentration of 10 nM. Protein, inhibitor and probe were combined and incubated for 15 min prior to analysis. Polarized fluorescence was plotted against concentration and fitted using a standard dose response curve. K_i values were calculated using the formula below where [STAT3] = 150 nM and K_d = 150 nM.

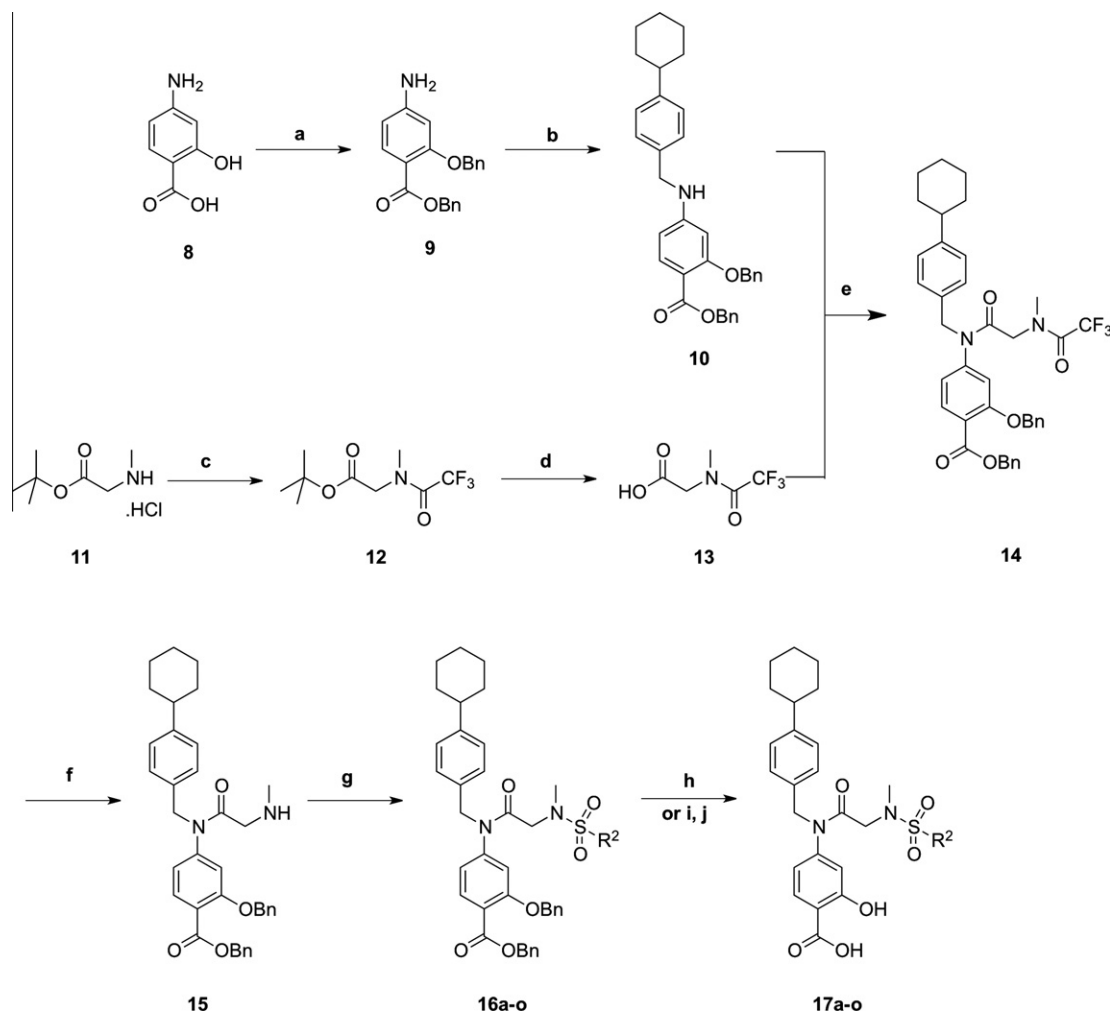
$$K_i = \frac{IC_{50}}{1 + \frac{[STAT3]}{K_d}}$$

Whole cell cytotoxicity assays: Human cell lines, DU145, OCI-AML2 and JJN3 were prepared in 96 well plates and treated with varying concentration of inhibitor. After 72 h, cell growth and viability was measured with the CellTiter96 aqueous non-radioactive (MTS) assay according to the manufacturer's instructions (Promega, Madison, WI) and as described previously.²² Relative viability was plotted versus concentration and EC₅₀ was determined by fitting to a standard dose response curve.

Immunoblotting: Cells were lysed in lysis buffer (50 mM Tris-HCl, 1 mM EDTA, 1% NP-40, 150 mM NaCl) for 30 min on ice, then freeze/thaw once at -80 °C and clarified by centrifugation at 12000g for 15 min. Proteins were separated by 6.5–15% sodium dodecyl-polyacrylamide gel electrophoresis (SDS-PAGE) and immunoblotted with the specified antibody. Protein bands were visualized using secondary antibodies coupled to horseradish peroxidase and the Chemiluminescence Reagent Plus (from Perkin Elmer Life Sciences) according to the manufacturer's instructions. Anti-cMyc was purchased from Santa Cruz, anti-survivin from NOVUS Biologicals, Anti-Mcl-1, and anti-Bcl-xL from BD Biosciences, (Mississauga, ON), anti-phospho STAT3, anti-STAT3 and anti-PARP are from Cell Signaling Technology, (Pickering, ON).

Results and discussion: A family of 16 novel sulfonamide analogs of **7** were prepared as outlined in Scheme 1. Briefly, 4-aminosalicylic acid (**8**) was doubly benzylated in one pot using potassium tert-butoxide and benzyl bromide. Next, aniline **9** was reductively aminated with 4-cyclohexylbenzaldehyde using NaCNBH₃. In parallel, we TFA protected the amino group of sarcosine *tert*-butyl ester (**11**) to furnish **12**, and then removed the *tert*-butyl ester under acidic conditions (TFA/CH₂Cl₂) to yield the carboxylic acid, **13**. Condensation of **13** with secondary aniline **10** furnished tertiary amide, **14**. The TFA protecting group was then removed by LiOH mediated hydrolysis revealing secondary amine, **15**. In the penultimate step we coupled a diverse variety of sulfonyl chlorides to **15**, yielding compounds, **16a–o**. Finally, hydrogenolysis conditions (H₂, 10% Pd/C) were employed to debenzylate the salicylic acid moiety, exposing final compounds **17a–o**. Of note, in cases where hydrogenolysis conditions were incompatible with the sulfonyl substituent (**17f**, **17j**, **17k**, and **17n**), we employed a step-wise, TFA mediated debenzylation of phenol, followed by LiOH hydrolysis of the benzyl ester (Scheme 1, steps i and j).²³

We first assessed for inhibitor induced Stat3–Stat3 dimer disruption using a routinely used Electrophoretic Mobility Shift Assay (EMSA), which measures dimer disruption through inhibition of DNA binding.²⁴ As illustrated in Table 1, varying the sulfonamide substituent resulted in varying degrees of inhibition potency. We incorporated a range of appendages to cater for the relatively amphiphilic pocket composed of residues Ile634, Ser636, Glu594 and the hydrophobic chain of Lys591. In general, hydrophobic R groups afforded the most potent inhibitors. The polar **17h**, incorporating a 1-methyl-1H-imidazole group, lost all inhibitory potency (IC₅₀ >300 μM). Interestingly, employing the *meta*-tolyl isomer **17a** significantly reduced activity, (**17a** (*meta*-) IC₅₀ = 118.8 μM cf. **7** (*para*-) IC₅₀ = 35 μM). The bulkier 2,4,6-tri-methylphenyl substituted inhibitor, **17b** exhibited weaker activity than the parent compound **7**, with an IC₅₀ = 51.9 μM. The larger biphenyl sulfonamide, **17c**, was a modest inhibitor of Stat3 dimerization



Scheme 1. Reagents and conditions: (a) BnBr (2 equiv), KO^tBu, DMF, 0 °C, 16 h, 73%; (b) 4-cyclohexylbenzaldehyde, AcOH, NaCNBH₃, rt, 16 h, 79%; (c) (CF₃CO)₂O, DIPEA, CH₂Cl₂, rt, 3 h, 96%; (d) TFA/CH₂Cl₂, 1:1, rt, 5 h, 100%; (e) **10**, PPh₃Cl₂, CHCl₃, 60 °C, 12 h, 97%; (f) LiOH·H₂O, THF/H₂O, 3:1, rt, 10 min, 98%; (g) RSO₂Cl, DIPEA, CH₂Cl₂, rt, 16 h, 78–98%; (h) H₂, 10% Pd/C, MeOH/THF, 1:1, rt, 1–16 h, 85–100%; or for **17f**, **17j**, **17k**, and **17n**: (i) LiOH·H₂O, THF/H₂O, 3:1, rt, 24 h, 73–89%; (j) TFA / CH₂Cl₂, 1:2, rt, 16 h, 65–92%.

(IC₅₀ = 65.4 μM), as was the 2-naphthyl derivative, **17d** (IC₅₀ = 79.2 μM). Notably, bis-aryl sulfonyl derivatives substituted at the 1-position, including, **17e** (R = 1-naphthyl, IC₅₀ = 28.8 μM), **17f** (R = 8-quinolyl, IC₅₀ = 25 μM) and **17g** (R = dansyl, IC₅₀ = 29 μM) proved to be active Stat3 inhibitors. Taken together, these data suggest that substitution of the *ortho*- and *meta*-tolyl positions of **7**, with a second aryl group is better tolerated than in the *para* position. In general, replacement of the methyl group in the *para*-tolyl moiety of **7** with different isosteres (F, Br, Cl, OMe, NO₂) led to a reduction in Stat3 inhibitory activity. However, **17o**, incorporating a pentafluorophenyl sulfonamide substituent, proved to be the most active of the phenyl sulfonamide series. Indeed, **17o** was approximately 2-fold more potent as the parent compound **7** (IC₅₀ = 19 μM cf. **7**, IC₅₀ = 35 μM).

Next, we investigated the binding potency of select agents against Stat3's SH2 domain via a routinely used fluorescence polarization assay, the results of which are shown in Table 2. Encouragingly, compounds **17b** (K_i = 8.0 μM), **17c** (K_i = 6.2 μM), **17g** (K_i = 13.3 μM), **17k** (K_i = 11.0 μM) and **17o** (K_i = 12.8 μM) exhibited improved activity compared to compound **7**. Although similar trends were observed in the EMSA and FP data, there are some notable deviations between the two data sets of data. For example, compound **17b**, IC₅₀ = 51.9 μM in the EMSA assay is significantly more potent in the FP assay (K_i = 8.0 μM). As previously reported,⁶ this anomaly between EMSA analysis of nuclear extracts, and the FP assay is likely due to the presence of other Stat isoforms and

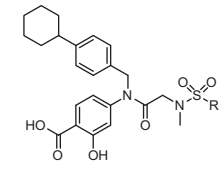
proteins found in the nuclear extracts. Taken together, the EMSA and FP results suggest that we are able to disrupt Stat3-phosphopeptide and Stat3-Stat3 complexation events by effectively blocking the Stat3 SH2 domain.

Since blockage of Stat3 signaling in compromised cell lines leads to induced apoptosis,²⁵ we reasoned that our most potent inhibitors would kill cells harboring activated Stat3. Thus, we employed an MTS assay to assess the whole cell potency of select inhibitors including, **7**, **17e**, and **17o**, which showed activity in both EMSA and FP-assays.^{26,27} DU145 (prostate), MDA-468 (breast) and JJN3 (multiple myeloma) cancer cells were incubated for 72 h with varying concentrations of inhibitors and relative viability assessed colorimetrically after treatment with MTS for 3 h. Notably, compound **17o** displayed an approximately 2-fold increase in potency over **7**, with IC₅₀ values of 10, 23, and 17 μM in breast, prostate and MM cells, respectively (Table 3). Compound **17e** showed lower activity in cells than both **7** and **17o**, possibly a result of increased lipophilicity and poorer water solubility (**17e**, log P = 5.95 vs **17o**, log P = 5.74). We noted that **17o** exhibited much improved water solubility over both **7** and **17e**. While the *in vitro* activities of **17o** and **7** are comparable, we postulated that the resultant increase in cellular activity may be a result of greater cell permeability and reduced aggregation/precipitation.

Due to the promising cytotoxic activity observed in tumor cells, **17o** was assayed for inhibition of Stat3 phosphorylation in both MDA-468 and JJN3 cell lines harboring activated Stat3 (Fig. 3).^{28,29}

Table 1

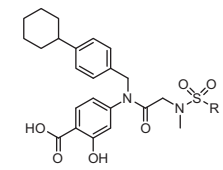
EMSA inhibition data for the disruption of the Stat3–Stat3–DNA complex by sulfonamide analogs **7** and **17a–17o**



Inhibitor	R	IC ₅₀ (μM)	Inhibitor	R	IC ₅₀ (μM)
7		35 ± 9	17h		>300
17a		118.8 ± 1.9	17i		126.2 ± 5.3
17b		51.9 ± 2.4	17j		90.3 ± 4.5
17c		65.4 ± 7.1	17k		67.2 ± 2.6
17d		79.2 ± 11.2	17l		>300
17e		28.8 ± 2	17m		67.4 ± 4.9
17f		24.6 ± 3.4	17n		62.2 ± 3.2
17g		28.8 ± 1.9	17o		19.7 ± 5.4

Table 2

Fluorescence polarization assay binding data (K_i values in μM)

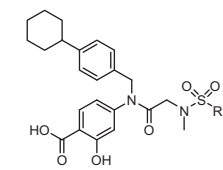


Inhibitor	R	K _i (μM)	Inhibitor	R	K _i (μM)
7		15.5 ± 4.7	17g		13.3 ± 0.6
17b		8.0 ± 2.4	17h		>100
17c		6.2 ± 2.0	17i		30.6 ± 11
17e		26.5 ± 0.4	17k		11.0 ± 0.3
17f		41.0 ± 0.4	17o		12.8 ± 0.3

As a control, Western blot analysis showed that control inhibitor, **7** effectively knocked down Stat3 phosphorylation at approximately 100 μM in both MDA-468 and JJN3 cancer cells. Most encouragingly, **17o** inhibited Stat3 phosphorylation at significantly lower concentrations (20 μM) in intact cells after 24 h. Furthermore, immunoblotting analysis of the same cell lines after the same time

Table 3

Whole cell MTS data. Cells were treated with varying concentrations of inhibitors for 72 h



Inhibitor	R	MDA-468	EC ₅₀ (μM)	DUI 45	JJN3
7		17.0 ± 4.4	37.2 ± 12.4		93.3 ± 15.8
17e		46.5 ± 12.4	74.5 ± 30.2		106. ± 13.7
17o		10.9 ± 3.0	22.7 ± 8.5		16.7 ± 0.7

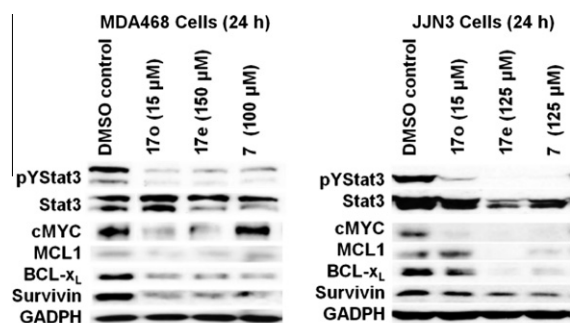


Figure 3. SDS–PAGE and Western blotting analysis of whole cell lysates prepared from MDA-468 human breast cancer and multiple myeloma JJN3 cells, untreated (DMSO, control) or treated with **17o** (15 μM), **17e** (125 or 150 μM), and **7** (100 or 125 μM) for 24 h and subjected to immunoblotting analysis for pY705Stat3, Stat3, c-Myc, Bcl-xL, Mcl-1 and Survivin.

period revealed that **17o** effectively reduced levels of Stat3 downstream targets, including, cMYC, Bcl-xL and Survivin. We presume that the resultant cytotoxicity observed after 72 h incubation is a result of **17o/7**-induced inhibition of intracellular Stat3 signaling. The data shows that **17o** is a more potent whole cell inhibitor of Stat3 function than lead compound, **7**, presumably due to improved solubility and cell permeability. We will conduct further investigations to elucidate the biological and biochemical mechanisms of **17o**'s improved anti-cancer activity which will be published elsewhere.

Conclusion: We have presented the design and synthesis of a novel family of Stat3 inhibitors that exhibit promising in vitro binding potency for the Stat3 SH2 domain, as well as improved tumor whole cell activity. Most notably, hit compound, **17o**, showed an approximately 2- to 4-fold increase in in vitro activity compared to lead agent, **7**, and nearly 6-fold higher potency in JJN3 MM tumor cells. Future studies seek to evaluate the in vivo properties of **17o** in MM and breast tumor xenograft models. Thus, to date, **17o** represents the most potent Stat3 inhibitor derived from the salicylic acid-based class of inhibitors.

Acknowledgments

This work was supported by NSERC (PTG), University of Toronto (PTG), Canadian Foundation for Innovation (PTG) and by the Na-

tional Cancer Institute Grants CA106439 (JT) and CA128865 (JT) and an Ontario Graduate Scholarship (BDGP). Aaron Schimmer is a Leukemia and Lymphoma Society Scholar in Clinical Research.

Supplementary data

Supplementary data (characterization of all chemical compounds and representative results from EMSA, FP and whole cell cytotoxicity assays) associated with this article can be found, in the online version, at doi:10.1016/j.bmcl.2011.06.056.

References and notes

1. Page, B. D. G.; Ball, D. P.; Gunning, P. T. *Exp. Opin. Ther. Pat.* **2011**, *21*, 65.
2. Fletcher, S.; Drewry, J. A.; Shahani, V. M.; Page, B. D. G.; Gunning, P. T. *Biochem. Cell Biol.* **2009**, *87*, 825.
3. Leonard, W. J. *Nat. Med.* **1996**, *2*, 968.
4. Herrington, J.; Carter-Su, C. *Trends Endocrin. Met.* **2001**, *12*, 252.
5. Darnell, J. E., Jr. *Science* **1997**, *277*, 1630.
6. Fletcher, S.; Singh, J.; Zhang, X.; Yue, P.; Page, B. D. G.; Sharmeen, S.; Shahani, V. M.; Zhao, W.; Schimmer, A. D.; Turkson, J.; Gunning, P. T. *ChemBioChem* **2009**, *10*, 1959.
7. Bromberg, J.; Darnell, J. E., Jr. *Oncogene* **2000**, *19*, 2468.
8. Bowman, T.; Garcia, R.; Turkson, J.; Jove, R. *Oncogene* **2000**, *19*, 2474.
9. Lai, S. Y.; Johnson, F. M. *Drug Resist. Update.* **2010**, *13*, 67.
10. Fletcher, S.; Turkson, J.; Gunning, P. T. *ChemMedChem* **2008**, *3*, 1159.
11. Schust, J.; Sperl, B.; Hollis, A.; Mayer, T. U.; Berg, T. *Chem. Biol.* **2006**, *13*, 1235.
12. Gunning, P. T.; Glenn, M. P.; Siddiquee, K. A.; Katt, W. P.; Masson, E.; Sebti, S. M.; Turkson, J.; Hamilton, A. D. *ChemBioChem* **2008**, *9*, 2800.
13. Siddiquee, K.; Zhang, S.; Guida, W. C.; Blaskovich, M. A.; Greedy, B.; Lawrence, H. R.; Yip, M. L. R.; Jove, R.; McLaughlin, M. M.; Lawrence, N. J.; Sebti, S. M.; Turkson, J. *Proc. Natl. Acad. Sci. U.S.A.* **2007**, *104*, 7391.
14. Turkson, J.; Kim, J. S.; Zhang, S.; Yuan, J.; Huang, M.; Glenn, M.; Haura, E.; Sebti, S.; Hamilton, A. D.; Jove, R. *Mol. Cancer Ther.* **2004**, *3*, 261.
15. Bhasin, D.; Cisek, K.; Pandharkar, T.; Regan, N.; Li, C.; Pandit, B.; Lin, J.; Li, P. K. *Bioorg. Med. Chem. Lett.* **2008**, *18*, 391.
16. Matsuno, K.; Masuda, Y.; Uehara, Y.; Sato, H.; Muroya, A.; Takahashi, O.; Yokotagawa, T.; Furuya, T.; Okawara, T.; Otsuka, M.; Ogo, N.; Ashizawa, T.; Oshita, C.; Tai, S.; Ishii, H.; Akiyama, Y.; Asai, A. A. C. S. *Med. Chem. Lett.* **2010**, *1*, 371.
17. Xu, X.; Kasembeli, M. M.; Jiang, X.; Twardy, B. J.; Twardy, D. J. *PLoS ONE* **2009**, *4*.
18. Fletcher, S.; Page, B. D. G.; Zhang, X.; Yue, P.; Li, Z. H.; Sharmeen, S.; Singh, J.; Zhao, W.; Schimmer, A. D.; Trudel, S.; Turkson, J.; Gunning, P. T. *ChemMedChem* **2011**, *In Press*, doi:10.1002/cmdc.201100194.
19. Zhang, X.; Yue, P.; Fletcher, S.; Zhao, W.; Gunning, P. T.; Turkson, J. *Biochem. Pharmacol.* **2010**, *79*, 1398.
20. Jones, G.; Willett, P.; Glen, R. C.; Leach, A. R.; Taylor, R. J. *Mol. Biol.* **1997**, *267*, 727.
21. Schust, J.; Berg, T. *Anal. Biochem.* **2004**, *330*, 114.
22. Simpson, C. D.; Mawji, I. A.; Anyiwe, K.; Williams, M. A.; Wang, X.; Venugopal, A. L.; Gronda, M.; Hurren, R.; Cheng, S.; Serra, S.; Zavareh, R. B.; Datti, A.; Wrana, J. L.; Ezzat, S.; Schimmer, A. D. *Cancer Res.* **2009**, *69*, 2739.
23. Fletcher, S.; Gunning, P. T. *Tetrahedron Lett.* **2008**, *49*, 4817.
24. Turkson, J.; Ryan, D.; Kim, J. S.; Zhang, Y.; Chen, Z.; Haura, E.; Laudano, A.; Sebti, S.; Hamilton, A. D.; Jove, R. *J. Biol. Chem.* **2001**, *276*, 45443.
25. Bromberg, J. *J. Clin. Invest.* **2002**, *109*, 1139.
26. Scudiero, D. A.; Shoemaker, R. H.; Paull, K. D.; Monks, A.; Tierney, S.; Nofziger, T. H.; Currens, M. J.; Seniff, D.; Boyd, M. R. *Cancer Res.* **1988**, *48*, 4827.
27. Alley, M. C.; Scudiero, D. A.; Monks, A.; Hursey Czerwinski, M. L. M. J.; Fine, D. L.; Abbott, B. J.; Mayo, J. G.; Shoemaker, R. H.; Boyd, M. R. *Cancer Res.* **1988**, *48*, 589.
28. Sartor, C. I.; Dziubinski, M. L.; Yu, C. L.; Jove, R.; Ethier, S. P. *Cancer Res.* **1997**, *57*, 978.
29. Brenne, A. T.; Ro, T. B.; Waage, A.; Sundan, A.; Borset, M.; Hjorth-Hansen, H. *Blood* **2002**, *99*, 3756.